

Application of relativistic Fock-space coupled-cluster theory to study Li and Li-like ions in plasmaMadhulita Das,^{1,*} Madhusmita Das,^{2,3} Rajat K. Chaudhuri,^{1,†} and Sudip Chattopadhyay^{4,‡}¹*Indian Institute of Astrophysics, Bangalore 560034, India*²*Department of Physics, Indian Institute of Technology, Bombay 400076, India*³*Theoretical Physics Division, Bhabha Atomic Research Centre, Mumbai 400085, India*⁴*Department of Chemistry, Bengal Engineering and Science University, Shibpur, India*

(Received 19 December 2011; published 5 April 2012)

The ionization potentials, transition energies, and oscillator strengths of Li and Li-like C^{3+} and Al^{10+} are computed at different plasma environments with the Fock-space multireference coupled-cluster theory to examine the parametric dependence of these properties on plasma density and/or temperature. The results presented here show that the ionization and transition energies as well as the oscillator strengths are very sensitive to the plasma environment. It further shows that the spectral lines corresponding to $\Delta n = 0$ transitions for Li-like C^{3+} and Al^{10+} are *blueshifted*, whereas the lines associated to $\Delta n \neq 0$ are *redshifted* (n is the principal quantum number).

DOI: [10.1103/PhysRevA.85.042506](https://doi.org/10.1103/PhysRevA.85.042506)

PACS number(s): 32.70.Cs, 31.15.xp, 31.15.bw

I. INTRODUCTION

Significant theoretical and experimental progress has been made over the last few years in explaining and predicting the spectral lines of atoms and ions embedded in plasma environment [1–15]. Despite considerable progress, interest in theoretical investigation of plasma screening effects on the electronic structures of ions has remained unabated over the years. In many physical systems of interest (e.g., laboratory or astrophysical plasma), matter exists in plasma form, pertaining to very high temperature ($T \sim$ eV–keV) and density ($n > 10^{21}$ cm⁻³). At such extreme conditions, plasma contains a variety of charged species and free electrons. The physical properties of plasma are very much dependent on the microscopic structure of its constituents (neutral to highly ionized ions). Therefore, the spectral properties of singly or multiply ionized atoms is of great importance for the diagnostics of laboratory plasmas as well as for the understanding of stellar spectra and atmospheric opacities. It is well known that the Coulomb attraction between nucleus and bound electrons of atoms or ions (embedded in plasma) is screened by the surrounding ions and fast electrons. This screening effect not only alters the spectral properties of atoms/ions immersed in plasma but also gives rise to phenomena such as pressure ionization and continuum lowering [16]. The variation of the energy levels of atoms or ions in plasma plays a key role in the study of radiation emitted from plasma, and hence, is important for plasma diagnostic purposes. The theoretical studies of atomic properties in dense plasmas can also provide useful information about the spectral line shifts, change in line profiles, etc., of the embedded species, which can subsequently be used in investigating the quantum fluid properties using sensitive external microprobes.

It is now widely accepted that an accurate description of the electronic structure along with various spectral properties of

atoms and ions immersed in plasma requires proper modeling of the plasma potential in addition to the balanced treatment of electron correlation effects. Modeling of the atomic or ionic potential under plasma environment is nontrivial. The simplest approach is to treat the repulsive interaction of the free electrons of plasma with the bound electrons which gives rise to a finite number of bound states for the ions. The choice of appropriate model potential depends on the coupling strength ($\Gamma = \frac{E_C}{E_T}$) of the plasma which is the ratio of Coulomb energy ($E_C = \frac{Z^2 e^2}{r_i}$) to thermal energy ($E_T = k_B T$). For weakly coupled plasma ($\Gamma < 1$: low density and high temperature), the screening of nuclear charge by free electrons of the plasma is modeled via Debye potential [17], whereas for a strongly coupled plasma ($\Gamma > 1$: high density and low temperature), the effect of screening as well as confinement by neighboring ions is described through ion-sphere (IS) potential [18].

The Debye and the ion-sphere potentials have been found to be the most simple and successful models in describing the atomic potential under plasma environment [1,2,19–22]. Bhattacharya *et al.* [23] have calculated the spectral properties of H- and He-like ions in strongly coupled plasma at the random-phase approximation (RPA) level with the IS model. Saha and Fritzsche [15] studied the changes of energy levels, oscillator strengths, and emission rates for a Be I isoelectronic sequence using the multiconfiguration Dirac-Fock (MCDF) method. Recently, Li *et al.* [24] investigated the influence of hot and dense plasmas by invoking the average-atom model on energy levels and oscillator strengths of beryllium-like ions for $Z = 26$ –36, over a wide range of temperatures and densities using the self-consistent-field multiconfiguration Dirac-Fock method. It is pertinent to note that transition energies and related properties reported in most of these investigations were carried out in a nonrelativistic framework with some exceptions [25]. At this juncture we reiterate that the relativistic corrections on the plasma screening are very useful for interpretation of the spectral lines, especially for the highly charged ions. Recently, Das *et al.* [26] studied the effect of plasma environment on the ionization potential and excitation energies of He-like (C^{4+} , Al^{11+} , and Ar^{16+}) ions

*Corresponding author: madhulita@iiap.res.in

†Corresponding author: rkchaudh@iiap.res.in

‡Corresponding author: sudip_chattopadhyay@rediffmail.com

using the relativistic coupled cluster linear response theory (CCLRT) [27]. In passing, we note that for specific temperature (T) and density (ρ), attainable in the laboratory, Li-like ions are the most abundant charge species in plasma. For example, at $k_B T \sim 300$ eV and $\rho \sim 0.1$ g/cm³, aluminum plasma ($n \sim 10^{21}$ /cm³) is dominated by an Al¹⁰⁺ charge state.

Our modest aim in this paper is to analyze the influence of the plasma screening on the Li and Li-like C³⁺ and Al¹⁰⁺ ions. The ionization potentials, excitation energies, and oscillator strengths of these systems are calculated using both Debye and ion-sphere potentials with Dirac-Fock orbitals at the Fock-space multireference coupled cluster (FS-MRCC) [28–32] level of theory. The transition energies obtained at the FS-MRCC level for the isolated (free) systems (as well as under plasma environment) are in excellent agreement with NIST data and with available theoretical results [33,34]. The present study shows that the total energy of the system increases with increasing plasma strength indicating the instability of the system. It further demonstrates that with an increase in screening (plasma density), the principal quantum number conserving (violating) transition lines of C³⁺ and Al¹⁰⁺ ions exhibit blue (red)shift.

II. THEORY

In this section we present a brief resumé of the various plasma models used to describe the effective screening of the Coulomb potential for the system present in the plasma. The presence of ions and free electrons in a plasma alters the potential experienced by the bound electrons. In the altered potential [$V_{\text{eff}}(r_i)$], many electron Dirac Hamiltonian for the atom or ion can be represented as

$$\hat{H} = \sum_{i=1}^{N_{\text{elec}}} [c\vec{\alpha}_i \cdot \vec{p}_i + \beta mc^2 + V_{\text{eff}}(r_i)] + \sum_{i < j}^{N_{\text{elec}}} \frac{e^2}{r_{ij}}, \quad (1)$$

where $V_{\text{eff}}(r_i)$ is the effective potential experienced by the i th electron. The model potentials for the weakly and strongly coupled plasmas are given by

$$V_{\text{eff}}^{\text{D}}(r_i) = -\frac{Ze^{-\mu r_i}}{r_i} \quad (\text{Debye}), \quad (2)$$

$$V_{\text{eff}}^{\text{IS}}(r_i) = \frac{(Z - N)}{2R} \left[3 - \left(\frac{r_i}{R} \right)^2 \right] \quad (\text{ion sphere}), \quad (3)$$

where Z , N , μ , and R represent the nuclear charge, the charge state of the ion, the Debye screening parameter, and the ion-sphere radius, respectively. The Debye screening parameter μ and the ion-sphere radius R are related to the ion density n_{ion} and plasma temperature T (only for μ) through the following expressions:

$$\mu = \left[\frac{4\pi(1 + Z)n_{\text{ion}}}{k_B T} \right]^{1/2}, \quad (4)$$

$$R = \left(\frac{3}{4\pi n_{\text{ion}}} \right)^{1/3}, \quad (5)$$

in which k_B denotes the Boltzmann constant.

The Debye potential is a long-range potential where vanishing boundary conditions are satisfied at infinity, whereas

in the ion-sphere model a finite boundary condition is imposed [$\psi(r)|_R = 0$] [35]. This boundary condition indirectly brings in the effect of external plasma confinement due to neighboring ions. In principle, electronic charge in a particular level also gets screened by the plasma electrons but the effect is negligible for small values of μ .

In this work, the relativistic FS-MRCC method (see Refs. [28,29] details) for one electron attachment process has been used to compute the ground- and excited-state energies (also the properties) of Li and Li-like ions. In the FS-MRCC scheme, the required wave function for the single valence (k) open-shell system is given by

$$|\Psi_k^{N+1}\rangle = \Omega a_k^\dagger |\Phi_0^N\rangle, \quad (6)$$

where a_k^\dagger is the k th valence electron creation operator and Φ_0^N is the N -particle closed-shell Dirac-Fock (DF) wave function. The wave operator Ω formally represents the mapping of the reference space Φ_0^N onto the target space Ψ_k^{N+1} . The CC equations are solved for various plasma potential to compute the required ground- and excited-state energies. The electric dipole transition matrix elements are also computed to determine the oscillator strengths. For computational simplicity the cluster operator is constrained to single and double excitation known as the coupled-cluster single double (CCSD) scheme.

The electric dipole transition probability $A_{f \rightarrow i}^{E1}$ (in s⁻¹) from an upper state (f) to a lower state (i) is determined by using the formula [36]

$$A_{f \rightarrow i}^{E1} = \frac{2.0261 \times 10^{18}}{\lambda^3(2J_f + 1)} S^{E1}, \quad (7)$$

where S^{E1} is the transition line strength for the electric dipole transition ($E1$) in a.u., λ is the transition wavelength in Å, and $(2J_f + 1)$ is the degeneracy of upper level (f).

$$S^{E1} = |\langle f|Z|i\rangle|^2, \quad (8)$$

where $\langle f|Z|i\rangle$ corresponds to the electric dipole matrix element. The absorption oscillator strength for allowed transition from a lower state (i) to an upper state (f) is given by [36]

$$f = 1.4992 \times 10^{-16} \frac{g_f}{g_i} \lambda^2 A_{f \rightarrow i}^{E1}, \quad (9)$$

where $g_f = (2J_f + 1)$ and $g_i = (2J_i + 1)$ are the degeneracy of the upper and lower levels, respectively.

III. RESULTS AND DISCUSSION

The ionization potentials and excitation energies (as well as oscillator strengths) of Li and Li-like C³⁺ and Al¹⁰⁺ ions are computed at the FS-MRCC level of theory with Debye and IS potentials. In order to check the accuracy and consistency of our results, the transition energies and oscillator strengths of the isolated Li, C³⁺ and Al¹⁰⁺ calculated at the FS-MRCC level are compared with the NIST [33] data in Tables I and II, respectively. As can be seen in Table I, the FS-MRCC estimated transitions of these systems are in excellent agreement with NIST values. The oscillator strengths

TABLE I. Excitation energies (a.u.) of isolated ($\mu = 0$) Li and Li-like C^{3+} and Al^{10+} ions obtained from the FS-MRCC method.

Levels	FS-MRCC			NIST		
	Li	C^{3+}	Al^{10+}	Li ^a	C^{3+} ^b	Al^{10+} ^c
$2s_{1/2}$	0	0	0	0	0	0
$2p_{1/2}$	0.0679	0.2937	0.8033	0.0679	0.2938	0.8020
$2p_{3/2}$	0.0679	0.2943	0.8315	0.0679	0.1943	0.8284
$3s_{1/2}$	0.1240	1.3803	9.2101	0.1240	1.3799	9.2058
$3p_{1/2}$	0.1410	1.4589	9.4356	0.1409	1.4582	9.4260
$3p_{3/2}$	0.1410	1.4591	9.4438	0.1409	1.4584	9.4340
$3d_{3/2}$	0.1425	1.4803	9.5186	0.1425	1.4802	9.5141
$3d_{5/2}$	0.1425	1.4803	9.5211	0.1425	1.4803	9.5160
$4s_{1/2}$	0.1639	1.8294	12.3361	0.1595	1.8287	12.3280

^aNIST [33] data for Li.^bNIST [33] data for C^{3+} .^cNIST [33] data for Al^{10+} .

obtained using the FS-MRCC method for $2s_{1/2} \rightarrow 2p_{1/2}$ and $2s_{1/2} \rightarrow 2p_{3/2}$ transitions in Al^{10+} are found to be 0.0374 and 0.0776, which also agree well with NIST data (0.0372 and 0.0772) (see Table II). Our estimated oscillator strengths for $2s_{1/2} \rightarrow 3p_{1/2}$ and $2s_{1/2} \rightarrow 3p_{3/2}$ transitions are 0.110 and 0.218, where the corresponding NIST values are 0.111 and 0.221, respectively.

After validating the accuracy and efficiency of the method for isolated systems, the calculations are carried out with different Debye screening parameters μ for the Li atom. The μ in the Debye model is a function of plasma density n_{ion} and temperature T [see Eq. (4)]. Starting from $\mu = 0$ (isolated case) one can generate various plasma conditions by varying n_{ion} and T . For Li plasma, the screening parameter μ ranges from 0.0 to 0.15 a.u., where $\mu = 0.15$ corresponds to $n_{\text{ion}} \sim 10^{22} \text{ cm}^{-3}$ at $T = 10^6 \text{ K}$. The variation of the ionization potentials of Li with μ are shown in Table III. The ground-state energies reported by Sahoo *et al.* [34] are also listed in this table for comparison.

The variations of ionization potential with respect to the Debye screening parameter are depicted in Fig. 1. A similar trend is also observed for Li-like C^{3+} and Al^{10+} ions. This phenomenon is unique to ions embedded in plasma environment and is termed *continuum lowering*. The excited-state energies of Li for different plasma screenings are shown in Fig. 2. It is evident from Fig. 2 that the higher excited states being loosely bound survive only for the weakly coupled system. It further shows that the μ value corresponding to the ionization limit of the $4s_{1/2}$ state is smaller than that of the $3s_{1/2}$, $3p_{1/2,3/2}$, and

TABLE III. Variation of the ionization potential (in a.u.) of Li with various Debye screening parameters μ .

μ	E_g (Li)	Sahoo <i>et al.</i> ^a
0.00	0.1981	0.1981
0.01	0.1880	0.1881
0.02	0.1783	0.1785
0.04	0.1599	0.1602
0.05	0.1512	0.1516
0.10	0.1125	0.1131

^aReference [34].

$3d_{3/2,5/2}$ levels. A similar trend was also observed by Hiroshi *et al.* [37] for a Li atom in Debye plasma. Figure 3 plots the variation of $2s \rightarrow 2p$ and $2s \rightarrow 3p$ transition energies of Al^{10+} against the Debye screening parameter μ where μ varies from 0.00 to 0.75 a.u. The figure shows that the spectral lines associated with the $\Delta n = 0$ ($\Delta n \neq 0$) transition are blue (red)shifted with increasing screening strength.

It is well known that the shift in the energy level of atoms and ions in plasma arises due to the electron screening and quantum confinement [6] for bound-state orbitals. The inner levels which are close to the nucleus experience comparably higher screening effects than those lying near the boundary region (see Fig. 4). The shift in the energy levels E_s caused by the screening is given by

$$E_s = E_{\mu=0} - E_{\mu \neq 0},$$

where $E_{\mu=0}$ and $E_{\mu \neq 0}$ are the energies of free and screened atoms and ions, respectively. Figure 4 clearly indicates that the effect of screening is more for the inner energy levels ($2s, 2p_{1/2,3/2}$) than for the outer energy levels ($3s, 3p_{1/2,3/2}, 3d_{3/2,5/2}$). It is also evident from the figure that the levels having the same principal quantum number have nearly the same screening effect. The quantum confinement (arises due to shifting of boundary condition) also adds a positive contribution to the bound-state energy. The quantum confinement effect is more significant for the high-lying energy levels than the low-lying ones (the inner levels remain practically unaffected by any change in potential occurring near the boundary region). Our study shows that the $2s \rightarrow 2p$ ($\Delta n = 0$) transition energies are *blueshifted* with increasing Debye screening parameter, whereas the $2s \rightarrow 3p$ ($\Delta n \neq 0$) transition energies are *redshifted* with increasing μ value. A similar trend was also observed for H-like ions in Debye plasma by Qi *et al.* [1] and for He-like C^{4+} in Debye plasma by Ray *et al.* [38]. This phenomena is a manifestation of

TABLE II. Oscillator strength (f) of isolated ($\mu = 0$) Li and Li-like C^{3+} and Al^{10+} ions obtained from the FS-MRCC method. The entries within the square brackets indicate the power of 10.

Transitions	FS-MRCC			NIST [33]		
	Li	C^{3+}	Al^{10+}	Li	C^{3+}	Al^{10+}
$2s_{1/2} \rightarrow 2p_{1/2}$	2.49[−1]	9.49[−2]	3.74[−2]	2.4899[−1]	9.52[−2]	3.72[−2]
$2s_{1/2} \rightarrow 2p_{3/2}$	4.98[−1]	1.90[−1]	7.76[−2]	4.9797[−1]	1.90[−1]	7.72[−2]
$2s_{1/2} \rightarrow 3p_{1/2}$	1.57[−3]	6.69[−2]	1.10[−1]	1.570[−3]	6.78[−2]	1.11[−1]
$2s_{1/2} \rightarrow 3p_{3/2}$	3.13[−3]	1.34[−1]	2.18[−1]	3.14[−3]	1.36[−1]	2.21[−1]

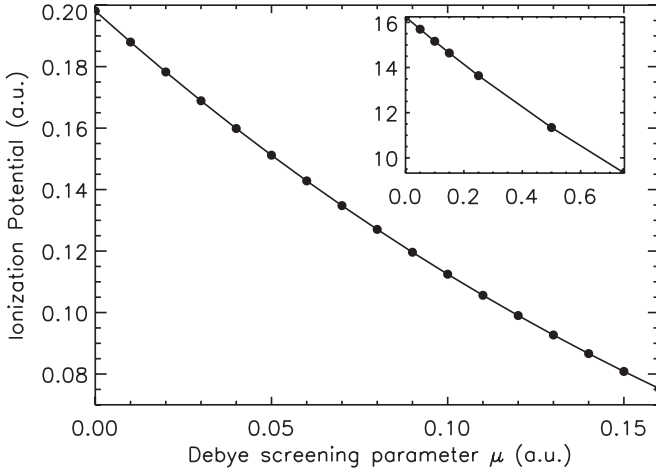


FIG. 1. Variation of ionization potential with Debye screening parameter μ (a.u.) for a Li atom. The inset plot is for the Al^{10+} ion.

the quantum confinement effect. This is also evident as our study shows that the higher angular momentum (l) energy levels having the same principal number (n) experience greater quantum confinement effect. For instance, the screening effect is roughly the same for the $2s$ and $2p_{1/2,3/2}$ levels, but the quantum confinement effect is more for the $2p$ ($l = 1$) level than for the $2s$ ($l = 0$) level.

The variations of the oscillator strength of Li for the $2s_{1/2} \rightarrow 2p_{[1/2,3/2]}$ and $2s_{1/2} \rightarrow 3p_{[1/2,3/2]}$ transitions (Table IV) are shown in Figs. 5(a) and 5(b) which demonstrate that the oscillator strength for the $2s_{1/2} \rightarrow 2p_{[1/2,3/2]}$ transition increases as μ increases, whereas the oscillator strength for the $2s_{1/2} \rightarrow 3p_{[1/2,3/2]}$ transition decreases with increasing plasma screening. It is worth mentioning that a similar trend is also observed for spectral lines of the Li-like Al^{10+} ion. Note that the value of the oscillator strength for an isolated ($\mu = 0$) atom or ion is unique but depends on μ in plasma environment. Figures 5(c) and 5(d), respectively, represent the screening effect on the oscillator strength for the $2s_{1/2} \rightarrow 2p_{[1/2,3/2]}$ and $2s_{1/2} \rightarrow 3p_{[1/2,3/2]}$ transitions of Al^{10+} . For the $2s \rightarrow 2p$

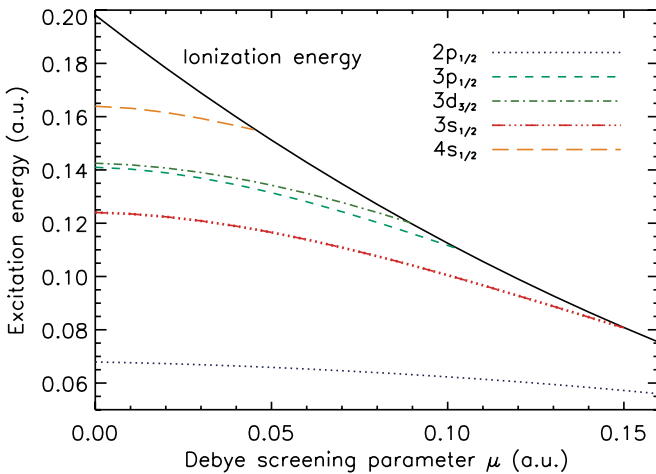


FIG. 2. (Color online) Variation of excitation energies of a Li atom with Debye screening parameter μ (a.u.).

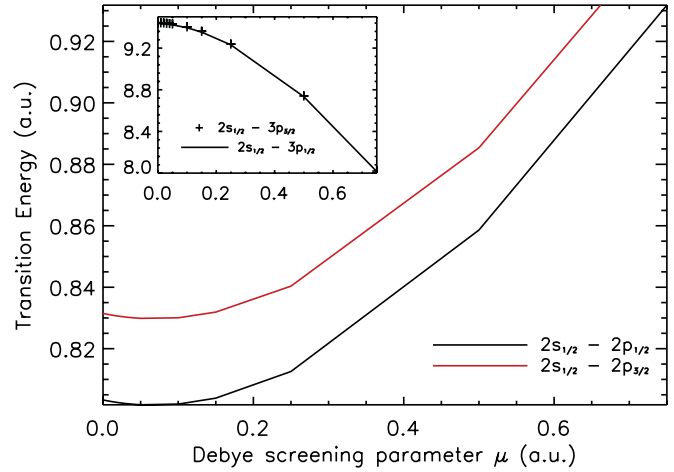


FIG. 3. (Color online) Variation of transition energies of Al^{10+} for a $\Delta n = 0$ transition. The inset plot is for the $\Delta n \neq 0$ transition.

($2s \rightarrow 3p$) transition, it increases (decreases) with μ . The enhancement in oscillator strength can be attributed to the larger radial overlap between the $2s$ and $2p$ states.

Finally, we address the variation of spectral properties of C^{3+} and Al^{10+} ions predicted by the IS model. Figure 6 depicts the variation of ionization energies of C^{3+} and Al^{10+} with ion density ($n_{\text{ion}} \sim 10^{21}/\text{cm}^3 \rightarrow 10^{23}/\text{cm}^3$). Our investigation shows that the ionization energy decreases monotonically with increasing ion density. The $2p_{[1/2,3/2]}-2s_{1/2}$ and $3p_{[1/2,3/2]}-2s_{1/2}$ transition energies are plotted against ion-sphere radius in Fig. 7. As can be seen in Fig. 7, there is an initial depletion in the $2p_{[1/2,3/2]}-2s_{1/2}$ and $3p_{[1/2,3/2]}-2s_{1/2}$ transition energies with increasing ion-sphere radius and remains constant for $R \geq 10$ a.u. It further shows that the $2p_{[1/2,3/2]}-2s_{1/2}$ and $3p_{[1/2,3/2]}-2s_{1/2}$ transition energies are shifted by the same amount with increasing ion-sphere radius. This is anticipated as the screening potential $V_{\text{eff}}^{\text{IS}} \rightarrow 0$ for large R , i.e., in the low-density regime ($V_{\text{eff}}^{\text{IS}} \propto \frac{1}{R}$). In passing, we note that similar behavior of transition energy with increasing ion density is also exhibited by the Li-like C^{3+} ion.

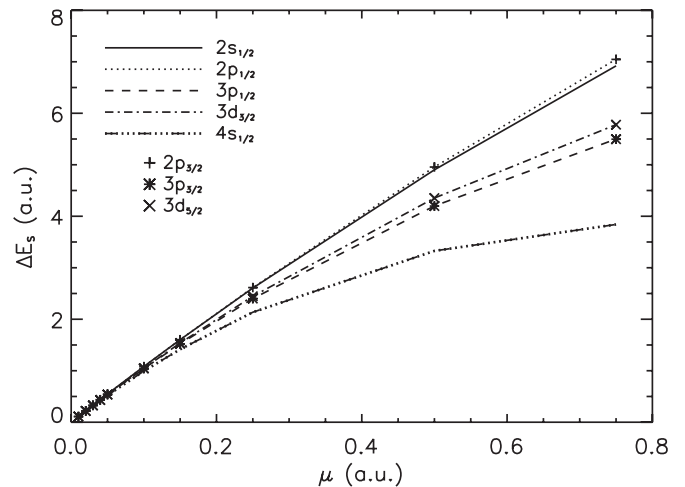


FIG. 4. Effect of screening on various energy levels of Al^{10+} .

TABLE IV. Oscillator strengths (f) of Li for different transitions with different Debye screening parameters μ . The numbers in square brackets indicate the power of 10.

μ (a.u.)	$2s_{1/2} \rightarrow 2p_{1/2}$	$2s_{1/2} \rightarrow 2p_{3/2}$	$2s_{1/2} \rightarrow 3p_{1/2}$	$2s_{1/2} \rightarrow 3p_{3/2}$
0.00	0.249	0.498	0.157[-2]	0.313[-2]
0.01	0.249	0.499	0.155[-2]	0.309[-2]
0.02	0.249	0.499	0.143[-2]	0.285[-2]
0.03	0.250	0.500	0.124[-2]	0.247[-2]
0.04	0.251	0.501	0.101[-2]	0.200[-2]
0.06	0.252	0.505	0.507[-3]	0.100[-2]
0.07	0.253	0.507	0.291[-3]	0.573[-3]
0.09	0.256	0.512	0.234[-4]	0.439[-4]
0.10	0.257	0.515	0.362[-5]	0.854[-5]
0.11	0.259	0.518		
0.13	0.262	0.524		
0.15	0.264	0.529		

IV. CONCLUDING REMARKS

The effect of plasma environment on the atomic structure of Li and Li-like C^{3+} and Al^{10+} are investigated using the FS-MRCC method. Both Debye and ion-sphere models have been used to study the effect of plasma on bound-bound transition properties of ions embedded in plasma. The computed results are compared with the available results in the literature. The results of the present work may be summarized by the following conclusions:

(1) It is found that the total energy of the system increases with increasing plasma strength indicating the instability of the system. Finally, for sufficient screening strength, the energy level merges into continuum.

(2) The most interesting result obtained from this work is, with an increase in screening (plasma density), $\Delta n = 0$ transition lines exhibit blueshift, whereas $\Delta n \neq 0$ yields redshift for Al^{10+} and C^{3+} . But for neutral lithium where the screening strength is small, all the transition energies show a decreasing trend with increasing screening strength.

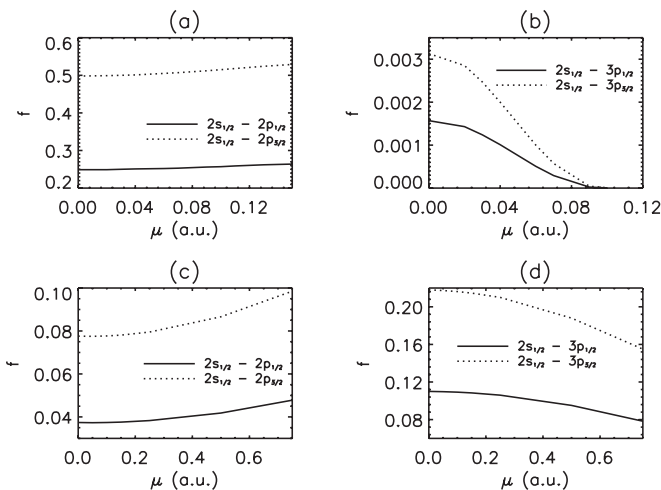


FIG. 5. Variation of oscillator strength with Debye screening parameter μ . Panels (a) and (b) correspond to the $2p-2s$ and $3p-2s$ transitions of the Li atom, respectively. Panels (c) and (d) correspond to $2p-2s$ and $3p-2s$ transitions of the Al^{10+} ion, respectively.

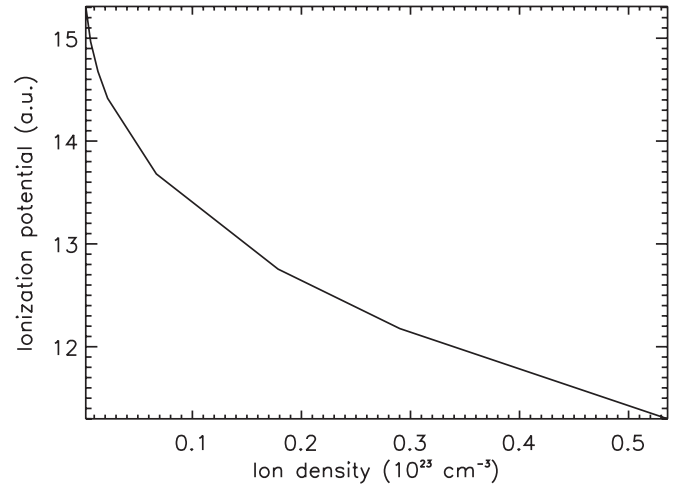


FIG. 6. Ionization potential of the Al^{10+} ion versus ion density in conjunction with the IS model.

(3) Both plasma screening and confinement play an important role in these principal quantum number conserving and nonconserving transitions in large screening strengths.

(4) Our results also show that the presence of plasma environments has a considerable effect on the oscillator strengths and transition probabilities of atoms and ions embedded in the plasmas.

Finally, our present findings would be very useful in the interpretation of spectral properties of Li and Li-like ions in laboratory and astrophysical plasmas. We are not in a position to argue that the relativistic FS-MRCC method is a superior method to study the many-electron systems in plasma environment for general use but it is certainly a potential one. For such a claim, more extensive applications of the method are called for. In the end, we hope that the present relativistic FS-MRCC calculation will open an avenue for accurate computation of properties of spectroscopic interest for small to large systems in weak and strong plasmas in the near future.

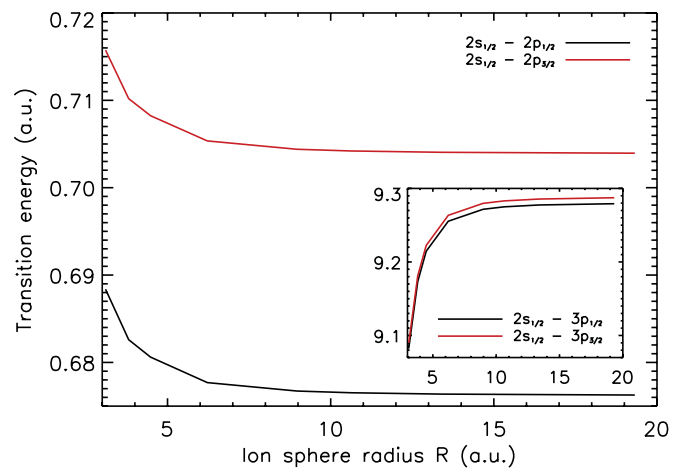


FIG. 7. (Color online) Change in $2p_{[1/2,3/2]}-2s_{1/2}$ transition energies of Al^{10+} with ion density by invoking the IS model. The inset plot is for $3p_{[1/2,3/2]}-2s_{1/2}$ transition energies of Al^{10+} with ion density.

ACKNOWLEDGMENTS

This work has been supported by the Department of Science and Technology, India (Grant No. SR/S1/PC-61/2009). M. D. is grateful to Dr. S. V. G. Menon (Theoretical Physics Division,

BARC, Mumbai) for many useful discussions throughout the course of this work. S.C. acknowledges the facilities developed in the Department of Chemistry, BESU, through UGC-SAP program.

-
- [1] Y. Y. Qi, J. G. Wang, and R. K. Janev, *Phys. Rev. A* **78**, 062511 (2008).
- [2] B. Saha, P. K. Mukherjee, D. Bielinska-Waz, and J. Karwowski, *J. Quant. Spectrosc. Radiat. Transf.* **92**, 1 (2005).
- [3] Carl A. Rouse, *Phys. Rev. A* **4**, 90 (1971).
- [4] C. Gao, J. Zeng, and J. Yuan, *High Energy Density Phys.* **7**, 54 (2011).
- [5] J.-Q. Pang, Guo-xing Han, Ze-qing Wu, and Shi-chang Li, *J. Phys. B* **35**, 2117 (2002).
- [6] Yongqiang Li, Jianhua Wu, Yong Hou, and Jianmin Yuan, *J. Phys. B* **41**, 145002 (2008).
- [7] F. J. Rogers and C. A. Iglesias, *Science* **263**, 50 (1994).
- [8] E. Storm, *J. Fusion Energy* **7**, 131 (1988).
- [9] G. Mourou and D. Umstadter, *Phys. Fluids. B* **4**, 2315 (1992).
- [10] J. Workman, M. Nantel, A. Maksimchuk, and D. Umstadter, *Appl. Phys. Lett.* **70**, 312 (1997).
- [11] M. M. Murnane, H. C. Kapreyn, M. D. Rosen, and R. W. Falcone, *Science* **251**, 531 (1991).
- [12] J. Seidel, S. Arndt, and W. D. Kraeft, *Phys. Rev. E* **52**, 5387 (1995).
- [13] D. Ray, *Phys. Rev. E* **62**, 4126 (2000).
- [14] T. C. Killian, T. Pattard, T. Pohl, and J. M. Rost, *Phys. Rep.* **449**, 77 (2007).
- [15] B. Saha and S. Fritzsche, *Phys. Rev. E* **73**, 036405 (2006).
- [16] D. Salzmann, *Atomic Physics in Hot Plasma* (Oxford University Press, Oxford, 1998).
- [17] M. S. Murillo and J. C. Weisheit, *Phys. Rep.* **302**, 1 (1998).
- [18] S. Ichimaru, *Rev. Mod. Phys.* **54**, 1017 (1982).
- [19] Y. Y. Qi, Y. Wu, J. G. Wang, and Y. Z. Qu, *Phys. Plasmas* **16**, 023502 (2009).
- [20] B. Saha, P. K. Mukherjee, and G. H. F. Dierksen, *Astron. Astrophys.* **396**, 337 (2002).
- [21] S. Paul and Y. K. Ho, *Phys. Plasmas* **16**, 063302 (2009).
- [22] J. K. Saha, S. Bhattacharyya, T. K. Mukherjee, and P. K. Mukherjee, *J. Phys. B* **42**, 245701 (2009).
- [23] S. Bhattacharya, A. N. Sil, and P. K. Mukherjee, *Eur. Phys. J. D* **46**, 1 (2008).
- [24] Y. Li, J. Wu, Y. Hou, and J. Yuan, *J. Phys. B* **41**, 145002 (2008).
- [25] J. K. Yuan, Y. S. Sun, and S. T. Zheng, *J. Phys. B* **28**, 457 (1995); **29**, 153 (1996); D. Bielinska-Waz, J. Karwowski, B. Saha, and P. K. Mukherjee, *Phys. Rev. E* **69**, 016404 (2004).
- [26] M. Das, R. K. Chaudhuri, S. Chattopadhyay, U. S. Mahapatra, and P. K. Mukherjee, *J. Phys. B* **44**, 245701 (2011).
- [27] D. Mukherjee and P. K. Mukherjee, *Chem. Phys.* **39**, 325 (1979).
- [28] D. Mukherjee, R. K. Moitra, and A. Mukhopadhyay, *Mol. Phys.* **30**, 1861 (1975); **33**, 955 (1977); I. Lindgren, *Int. J. Quantum Chem.* **S12**, 33 (1978); W. Kutzelnigg, *J. Chem. Phys.* **82**, 4166 (1985).
- [29] For a review on multireference CC methods and particularly the FS-MRCC approach, see I. Lindgren and D. Mukherjee, *Phys. Rep.* **151**, 93 (1987); D. Mukherjee and S. Pal, *Adv. Quantum Chem.* **20**, 292 (1989); U. Kaldor, *Theor. Chim. Acta* **80**, 427 (1991); for a review on relativistic FS-MRCC applications see U. Kaldor and E. Eliav, *Adv. Quantum Chem.* **31**, 313 (1998).
- [30] R. J. Bartlett and M. Musiał, *Rev. Mod. Phys.* **79**, 291 (2007).
- [31] D. Sinha, S. K. Mukhopadhyay, R. K. Chaudhuri, and D. Mukherjee, *Chem. Phys. Lett.* **154**, 544 (1989); S. Chattopadhyay, A. Mitra, and D. Sinha, *J. Chem. Phys.* **125**, 24411 (2006).
- [32] D. Mukhopadhyay, B. Datta, and D. Mukherjee, *Chem. Phys. Lett.* **197**, 236 (1992); L. Meissner and R. J. Bartlett, *J. Chem. Phys.* **102**, 7490 (1995); A. Landau, E. Eliav, and U. Kaldor, *Adv. Quantum Chem.* **39**, 171 (2001); E. Eliav, M. J. Vilkas, Y. Ishikawa, and U. Kaldor, *J. Chem. Phys.* **122**, 224113 (2005).
- [33] See [<http://physics.nist.gov/PhysRefData/ASD>].
- [34] S. Sahoo and Y. K. Ho, *Phys. Plasmas* **13**, 063301 (2006).
- [35] Balazs F. Rozsnyai, *Phys. Rev. A* **43**, 3035 (1991).
- [36] C. Sur, R. K. Chaudhuri, B. P. Das, and D. Mukherjee, *J. Phys. B* **38**, 4185 (2005).
- [37] H. Okutsu, T. Sako, K. Yamanouchi, and G. H. F. Dierksen, *J. Phys. B* **38**, 917 (2005).
- [38] D. Ray and P. K. Mukherjee, *J. Phys. B* **31**, 3479 (1998).